31st Annual International Conference of the IEEE EMBS
Minneapolis, Minnesota, USA, September 2-6, 2009

Finite Element Simulation of Ultrasound Propagation in Bone for Quantitative Ultrasound toward the Diagnosis of Osteoporosis

Sang-Hyuk Kim, *Student Member, IEEE*, Hyun Sang Suh, *Student Member, IEEE*, Min Hyoung Cho, Soo Yeol Lee, and Tae-Seong Kim, *Member*, *IEEE*

***Abstract*—Osteoporosis is a serious bone disease which leads to the increased risk of bone fractures. For prevention and therapy, early detection of osteoporosis is critical. In general, for diagnosis of osteoporosis, dual-energy X-ray absoptiometry (DXA) or densitometry is most commonly used. However DXA exhibits some disadvantages such as ionizing radiation, relatively expensive cost, and limited information on mineralization and geometry of the bone. As an alternative method of DXA, quantitative ultrasound (QUS) is being investigated. In contrast to DXA, QUS is non-ionizing and relatively inexpensive. It can also provide some bone-related parameters (e.g., quantitative measurements including speed of sound and frequency-dependent attenuation). However the estimation of these parameters is difficult and few analytical solutions exist due to the complex behavior of ultrasound propagation in bone. As an alternative to the analytical methods, in most attempts, finite difference time domain (FDTD) method is used for simulation of ultrasound propagation in bone with a limited capability of modeling complex geometries of the bone. Finite element method (FEM) is a better solution since it can handle the complex geometry, but has been rarely applied due to its computational complexity. In this work, we propose an approach of FEM-based simulation of ultrasound propagation in bone. To validate our approach, we have tested simulated and real bone models from micro-CT using the index of speed-of-sound. Our results achieve an average of 97.54% in the computational accuracy.**

I. Introduction

OSTEOPOROSIS is a bone disease caused by the loss in bone mass. Osteoporosis itself does not have specific symptoms but it leads to enhanced bone fragility, thereby increasing the risk of bone fractures. Considering hip fractures, at least 90% of which are caused by osteoporosis and only 15% of patients can walk without assistance and 50% of them never return to their normal state [1]. For fracture prevention and therapy, early detection of osteoporosis is essential.

Dual-energy X-ray absoptiometry (DXA) is the most commonly used device for the diagnosis of osteoporosis and it shows relatively good performance to assess bone mass and to detect bone fractures. However, DXA can only provide limited information on the mineralization and geometry of the bones in its 2-D projection mode. In addition, DXA has ionizing radiation and requires relatively high cost [2].

As an alternative method to DXA, an interest in quantitative ultrasound (QUS) is growing. In comparison to DXA, QUS is non-ionizing and relatively inexpensive. Furthermore, it can provide a variety of bone information and parameters because ultrasound propagation is subject to the structural and material properties of the propagation medium. Hence QUS offers good potentials to the early diagnosis of osteoporosis.

The main quantitative measurements are usually based on two ultrasound parameters such as speed of sound and frequency-dependent attenuation. These parameters are used under various approaches including ultrasound reflection, backscatter, transmission, and guided-wave propagation [3]. Nevertheless the relationship between these parameters on each approach and bone properties is not exactly understood yet and only few analytical solutions are available because the ultrasound propagation in bone shows complex behaviors depending on the geometrical complexity of the bone.

As an alternative to the analytical methods, numerical methods have been applied for the simulation of ultrasound propagation in bone. Especially finite difference time domain (FDTD) method is most widely used: for instance, the estimation of the bone mineral density at the distal radius [4], the simulation in the cortical bone [5], and the assessment of the sensitivity of QUS parameters in the cellular model [6]. This method is favorable due to its relatively simple implementation and good performance in some specific cases, but it suffers in modeling the complex structures of the bone due to its utilization of grid structure. In general, FDTD cannot be generalized for realistic simulation of ultrasound propagation in bone [2], [6].

In comparison to FDTD, finite element method (FEM) can handle complex geometries of the bone efficiently and adaptively based on its element flexibility. Also anisotropic properties of the bone can be handled well. Lately, the use of FEM is increasing as in ultrasound computed tomography [7], dental study [8], and brain surgery [9]. However there are rare studies of QUS through FE analysis.

In this paper, we have simulated ultrasound propagation in bone using FEM. In order to validate our approach, we have tested simple simulated bone models and real bone models derived from CT images. The derived index of time-of-flight is compared to the analytical solution. Our approach achieves an average accuracy of 97.54%.

Manuscript received April 7, 2009.

Sang-Hyuk Kim, Hyun Sang Suh, Min Hyoung Cho, Soo Yeol Lee and Tae-Seong Kim are with the Department of Biomedical Engineering, Kyung Hee University, Yongin, Gyeonggi, Republic of Korea (corresponding author to provide phone: +82-31-201-3731; fax: +82-31-201-3666; e-mail: tskim@khu.ac.kr).

II. Methods and Models

A. Mathematics for Ultrasound Propagation

We model the bone immersed in water. Hence there are two types of ultrasound propagation in our approaches. One propagates in water and the other propagates in bone. To simulate ultrasound propagation in water, the lossless wave equation is used, since ultrasonic waves attenuate little in water: the attenuation of water is considered as $0.0022\text{dB}\cdot\text{cm}^{-1}\cdot\text{MHz}^{-1}$ and in our model the distance between the transmitter and the receiver is short enough to neglect the attenuation.

The lossless ultrasonic wave equation is formulated as

$$\frac{1}{c^2}\frac{\partial^2 P}{\partial t^2} = \nabla^2 P \tag{1}$$

where c is the ultrasonic speed, P ultrasonic pressure, and t time. Ultrasonic speed in the fluid medium can be expressed as following:

$$c = \sqrt{\frac{k}{\rho}} \tag{2}$$

where ρ is the mean fluid density and k the bulk modulus of fluid.

The element matrices by discretization of the lossless wave equation are constructed using the Galerkin procedure and can be expressed as

$$[M_e^P]\{\ddot{P}_e\} + [K_e^P]\{P_e\} = 0 \tag{3}$$

where $[M_e^P]$ and $[K_e^P]$ are the fluid mass matrix and the fluid stiffness matrix respectively. The fluid mass matrix and the fluid stiffness matrix are given by

$$[M_e^P] = \frac{1}{c^2}\int_v \{N\}\{N\}^T dv \tag{4}$$

$$[K_e^P] = \int_v [B]^T [B] dv \tag{5}$$

where N is the shape function, [B] is $\{L\}\{N\}^T$, and {L} is a matrix operator defined as gradient or divergence operator [10].

For the simulation of ultrasound propagation in bone, the pressure of water is converted as the stress of bone at the interface between water and bone. The stress can be derived from the displacement of a particle. The relationship between the pressure and the displacement can be formulated as

$$\frac{\partial P}{\partial n} = -\rho\frac{\partial^2 u_n}{\partial t^2} \tag{6}$$

where n is the normal vector to the interface and u_n is a displacement vector normal to the interface. In the above equation, the pressure of water is a load which causes the acceleration of the bone.

By including conversion and damping at the boundary, (3) is rewritten as following:

$$[M_e^P]\{\ddot{P}_e\} + [C_e^P]\{\dot{P}_e\} + [K_e^P]\{P_e\} + \rho[R_e]^T\{\ddot{u}_e\} = 0 \tag{7}$$

where $[C_e^P]$ is the fluid damping matrix and $\rho[R_e]^T\{\ddot{u}_e\}$ fluid-structure coupling mass matrix derived from (6).

The absorbing boundary is applied to the whole models, resulting in no reflection at the boundary: hence ultrasound performs infinite propagation over the absorbing boundary.

B. Propagation in Simulated Bone

The first bone models are designed with a simple configuration in which a donut-shaped bone is immersed in water and two lines are set up to represent a transmitter and a receiver as shown in Fig. 1.

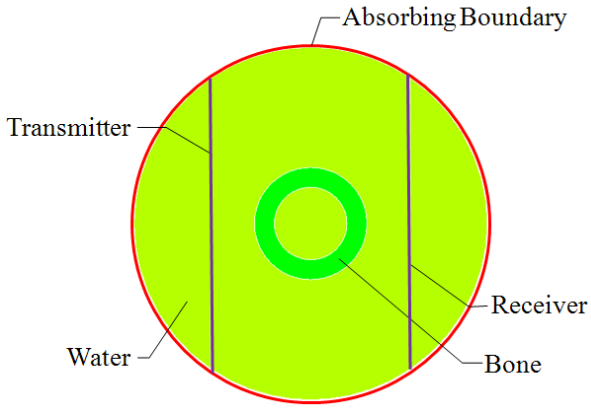

Fig. 1. Simulation configuration for a simple bone model.

The material properties are applied as follows: for water ρ=1000kg/m^3, c=1500m/s; for bone, ρ=1850kg/m^3, Young's modulus 8.6GPa and Poisson's ratio 4.28 [4]. In this setup, ultrasonic wave propagates in water as longitudinal waves and when it propagates in bone it shows both longitudinal and transverse waves. In bone, the longitudinal ultrasound speed is 2901m/s which is calculated by (2) with the Young's modulus and the transverse speed is 1307m/s, which is calculated with the shear modulus: shear modulus can be expressed as following

$$G = \frac{E}{2(1+v)} \tag{8}$$

where G is the shear modulus, E Young's modulus, and v Poisson's ratio.

As for the transmitter, 3kHz sinusoidal wave is emitted as the incident ultrasonic wave which is assumed as a plane wave. It is applied as a line source along the predefined transmitter as shown in Fig 1. In the case of real bone model, we apply 1MHz sinusoidal wave.

We carry out the transient analysis in ANSYS [12] for the ultrasound propagation simulation and have used the fluid29 and plane42 elements for water and bone. We set the time interval shorter than 1/20T of ultrasonic wave where T is the period of maximum frequency component of the incident wave, and set the element size smaller than at least 1/20 of the

minimum wavelength [10]. The water wavelength is calculated by the following equation.

$$\lambda = \frac{c}{f} \tag{9}$$

where λ is the wavelength and f is the frequency.

C. Propagation in Real Bone

The second real bone models are constructed using the bone images obtained with a micro-CT. The CT image reflects a cross-section of a rat femur as shown in Fig 2.

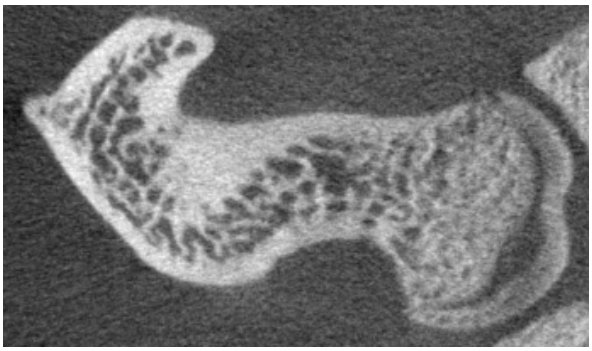

Fig. 2. A micro-CT image of the rat femoral bone.

The images are obtained with a zoom-in micro-CT which consists of a micro-focus x-ray source with a variable focal spot size of 5–50 um, a rotating subject holder with a rotation precision of 0.083°, and a CMOS flat-panel detector with a matrix size of 1248×1248 [11].

By applying a threshold, we segment out the bone regions, including the cortical and sponge bones, from the CT images and separate the bone area using some morphology operations. The whole model consisting of an arbitrary shaped bone which is immersed in water along with the transmitter and receiver is shown in Fig. 3.

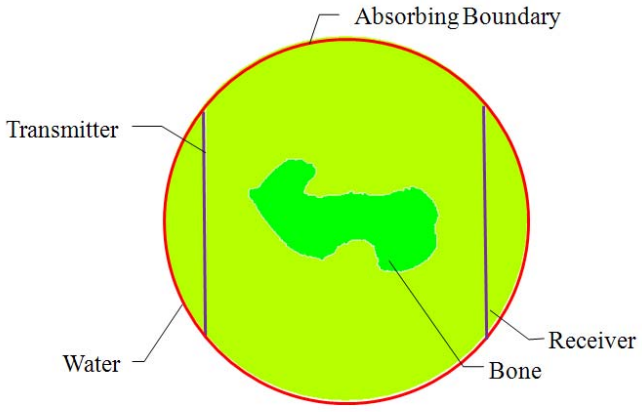

Fig. 3. Configuration for a real bone model

Fig.4 shows a mesh model of the segmented bone in green and bone marrow in red.

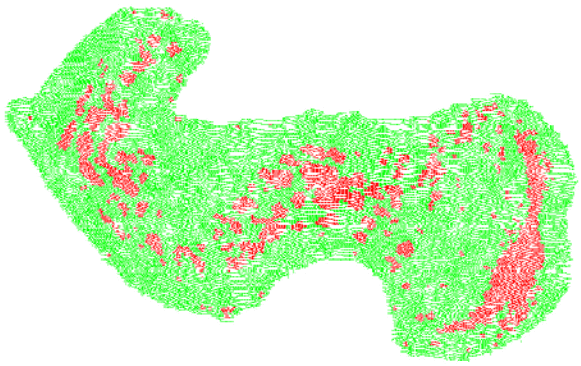

Fig. 4. A mesh model of the bone derived from a CT image.

The two properties of water and bone are same with the case of simple bone models. The material properties of bone marrow are defined as ρ=1030kg/m^3, and c=1540m/s calculated from the Young's modulus and Poisson's ratio according to (8). Consequently the applied properties for the bone marrow are E= 2.4GPa and v=0.45.

The type of incident ultrasonic wave from a line source is modeled as done in the simple type models: it is a sinusoidal wave with its center frequency of 1MHz.

We have performed the transient analysis with the time interval of 1/30T and the element size of 1/20 of its water wavelength.

III. Results and Discussion

In the case of simple bone model, we have changed the thickness of the bone (Case 1: 0.125m, Case 2: 0.225m, and Case 3: 0.32m) and simulated ultrasound propagation in each model to obtain the travel time. We have validated our FEM analysis via comparing the travel time obtained in the FEM results with the travel time calculated analytically.

The travel time in the FEM analysis is defined as the time interval between the maximum peaks of incident ultrasound and received ultrasonic waves. In each case, we obtain received ultrasounds at two positions which are the origin and the receiver along the horizontal axis.

Analytical travel times are calculated using the known information of the distance and the sound speed. All results are given in Table I in which the mean error is 2.1%.

For the real bone model, we have also simulated ultrasound propagation. Fig. 5 shows a series of propagating ultrasound waves. Fig. 6 shows the first arrival of the ultrasound wave, in which the waves along the horizontal axis arrives early due to the higher ultrasonic speed in bone than in water.

For validation, we analytically calculated the travel times of ultrasound waves propagating from the transmitter to the receiver along the horizontal axis in each case and then compare them with the FEM results. Consequently, the mean accuracy of FEM achieves 97.54% by considering both the simple bone type models and real-bone model.

TABLE I
Comparisons of Ultrasound Propagation Time

Condition		Analytical	Numerical	Error
Origin	Case 1	27.49ms	28.33ms	3.06%
	Case 2	25.49ms	25.00ms	1.90%
	Case 3	23.58ms	23.33ms	1.04%
	Mean (±Standard Deviation)			2.00 (±1.01)%
Receiver	Case 1	84.99ms	88.33ms	3.94%
	Case 2	80.97ms	80ms	1.20%
	Case 3	77.16ms	78.33ms	1.51%
	Mean (±Standard Deviation)			2.22 (±1.5)%

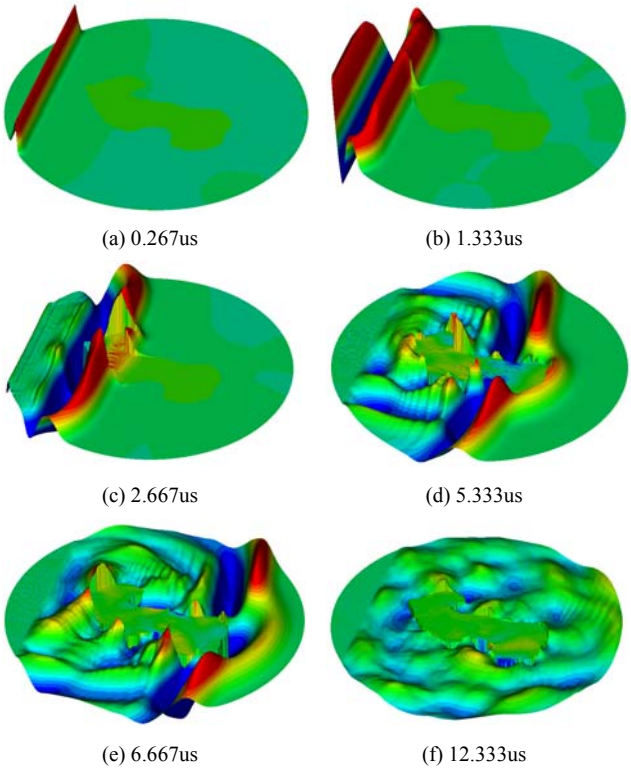

(a) 0.267us (b) 1.333us

(c) 2.667us (d) 5.333us

(e) 6.667us (f) 12.333us

Fig. 5. A time-series plot of propagating ultrasound waves in water and bone.

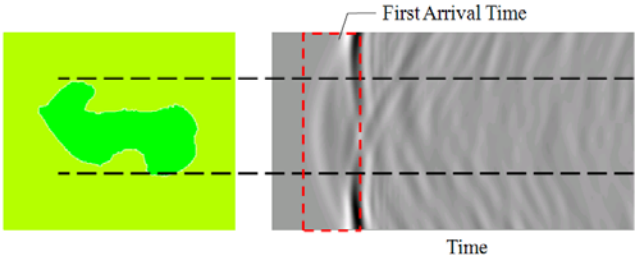

Fig. 6. Arriving ultrasound waves in the receiver region.

IV. Conclusion

In this paper, we have simulated ultrasound propagation in water and bone using the simple simulated bones and real bones via FEM. In comparison to FDTD, using FEM, we can model arbitrary shaped bones from CT images. We have validated our results by comparing our solutions against the analytical solutions. Our results show about the accuracy 97.54% in the wave travel time.

In this work, although the simulation study is carried out in 2D, it can be extended to 3D, allowing more realistic analysis of ultrasound propagation in bone. In addition, through FEM one can incorporate anisotropic bone properties and perform the analysis.

In conclusion, our preliminary results suggest the FEM approach can be an alternative yet a better tool for QUS with realistic representation of the bone geometries and anisotropic material properties.

Acknowledgment

This research was supported by MKE (Ministry of Knowledge Economy), Korea, under the ITRC (Information Technology Research Center) support program supervised by the IITA (Institute of Information Technology Advancement) (IITA-2009-(C1090-0902-0002)).

References

[1] D. Hans and M.-A. Krieg, "The clinical use of quantitative ultrasound (QUS) in the detection and management of osteoporosis," *IEEE Trans. Ultrason. Ferroelectr. Freq. Control.*, vol. 55, no.7, pp. 1529-1538, Jul. 2008.

[2] J. J. Kaufamn, G. Luo and R. S. Siffert, "Ultrasound simulation in bone," *IEEE Trans. Ultrason. Ferroelectr. Freq. Control.*, vol. 55, no. 6, pp. 1205-1218, Jun. 2008.

[3] P. Laugier, "Instrumentation for in vivo ultrasonic characterization of bone strength," *IEEE Trans. Ultrason. Ferroelectr. Freq. Control.*, vol. 55, no. 6, pp. 1179-1196, Jun. 2008.

[4] V. L. Floch, D. J. McMahon, G. Luo, A. Cohen, J. J. Kaufman, F. Shane and R. S. Siffert, "Ultrasound simulation in the distal radius using clinical high-resolution peripheral-CT images," *Ultrasound in Med. & Biol.*, vol. 34, no. 8, pp. 1317-1326, 2008.

[5] E. Bossy, M. Talmant and P. Laugier, "Three-dimensional simulations of ultrasonic axial transmission velocity measurement on cortical bone models," *J. Acoust. Soc. Amer.*, vol. 115, no. 5, pp. 2314-2324, 2004.

[6] G. Haiat, F. Padilla and P. Laugier, "Sensitivity of QUS parameters to controlled variations of bone strength assessed with a cellular model," *IEEE Trans. Ultrason. Ferroelectr. Freq. Control.*, vol. 55, no. 7, pp. 1205-1218, Jul. 2008.

[7] D. Hemzal, I. Peterlik, J. Rolecek, J. Jan, N. Ruiter and R. Jirik, "3D simulation of diffraction in ultrasonic computed tomography," in *Proc. 30th Annu. Int. Conf. IEEE EMBS*, Vancouver, 2008.

[8] X. Sun, E. A. witzel, H. Bian and S. Kang, "3-D finite element simulation for ultrasonic propagation in tooth," *Journal of Dentistry*, pp. 546-553, 2008.

[9] S. Behnia, A. Jafari, F. Ghalichi and A. Bonabi, "Finite-element simulation of ultrasound brain surgery: effects of frequency, focal pressures, and scanning path in bone-heating reduction," *Cent. Eur. J. Phys.*, pp. 211-222, 2008.

[10] W. D. O'Brein and Y. Liu, "Evaluation of acoustic propagation paths into the human head," *Air Force Office of Scientific Research*, 2005.

[11] I. K. Chun, M. H. Cho, J. H. Park and S. Y. Lee, "In vivo trabecular thickness measurement in cancellous bones: longitudinal rat imaging studies," *Physiol. Mears.*, vol. 27, pp. 695-702, 2006.

[12] ANSYS, Available: http://www.ansys.com/